

Holonomic gradient method for distribution function of a weighted sum of noncentral chi-square random variables

Tamio Koyama^{*†} and Akimichi Takemura^{*}

August, 2015

Abstract

We apply the holonomic gradient method to compute the distribution function of a weighted sum of independent noncentral chi-square random variables. It is the distribution function of the squared length of a multivariate normal random vector. We treat this distribution as an integral of the normalizing constant of the Fisher-Bingham distribution on the unit sphere and make use of the partial differential equations for the Fisher-Bingham distribution.

Keywords and phrases: algebraic statistics, cumulative chi-square distribution, Fisher-Bingham distribution, goodness of fit

1 Introduction

The weighted sum of independent chi-square variables appears in many important problems in statistics. In the problems for testing against ordered alternatives, cumulative chi-square statistic (cf. [7], [13]) has a good power. For studying the power function of the cumulative chi-square statistic, we need to evaluate the distribution function of a sum of weighted independent *noncentral* chi-square variables. Goodness of fit test statistics based on empirical cumulative distribution function, such as the Cramér-von Mises statistic or the Anderson-Darling statistic ([1]), are infinite sums of weighted independent chi-square variables. Chapter 4 of [4] gives a survey of these statistics. Under an alternative hypothesis the chi-square variables are noncentral. For studying the power function of these statistics we want to approximate the infinite sum by a finite sum of sufficiently many terms and compute the cumulative distribution of the finite sum.

An exact evaluation of the cumulative distribution function of a weighted sum of independent noncentral chi-square random variables was considered to be a difficult numerical problem (see [2]). Although the moment generating function is explicitly given, its Fourier inversion to evaluate the density function and the cumulative distribution function is difficult as extensively discussed in Chapter 6 of [16]. See [3] for the similar problems in other areas of applied mathematics.

Recently in [14] we proposed the holonomic gradient method (HGM) for calculating distribution functions and the maximum likelihood estimates using differential equations satisfied by a probability density function with respect to the parameters. Since then the method has been

^{*}Graduate School of Information Science and Technology, University of Tokyo

[†]Research Fellow of Japan Society for the Promotion of Science

successfully used in many problems, including the computations related to the Fisher-Bingham distribution on the unit sphere ([10], [8], [9], [15]). In this paper we utilize the results on HGM for the Fisher-Bingham distribution to evaluate the distribution function of a weighted sum of noncentral chi-square random variables.

Let \mathbf{X} denote a d -dimensional random vector following the multivariate normal distribution $N(\mu, \Sigma)$. Consider the cumulative distribution function $G(r)$ of $\|\mathbf{X}\|$:

$$G(r) = \int_{x_1^2 + \dots + x_d^2 \leq r^2} \frac{1}{(2\pi)^{d/2} |\Sigma|^{1/2}} \exp\left(-\frac{1}{2}(\mathbf{x} - \mu)^\top \Sigma^{-1}(\mathbf{x} - \mu)\right) d\mathbf{x}. \quad (1)$$

We call $G(r)$ the ball probability with radius r . By rotation we can assume that $\Sigma = \text{diag}(\sigma_1^2, \dots, \sigma_d^2)$ is a diagonal matrix without loss of generality. Hence $G(r)$ is the distribution function of the square root of a weighted sum of independent noncentral chi-square random variables, where weights are σ_i^2 , $i = 1, \dots, d$. Furthermore the conditional distribution of \mathbf{X} given its length $r = \|\mathbf{X}\|$ is the Fisher-Bingham distribution. This fact allows us to directly apply the results for the Fisher-Bingham distribution to the evaluation of the distribution of the weighted sum of independent noncentral chi-square random variables. As we show in Section 4 our method works very well, both in accuracy and speed.

The organization of this paper is as follows. In Section 2 we summarize known results on HGM for the Fisher-Bingham distribution and show how they can be used to evaluate the distribution of the a weighted sum of independent noncentral chi-square random variables. We also discuss the problem of initial values needed to use HGM. In Section 3 we present asymptotic results for the Fisher-Bingham integral and its derivatives for the case that the length of the multivariate normal vector diverges to infinity. This result is used to check the the numerical accuracy of our experiments in Section 4. We end the paper with some discussions in Section 5.

Acknowledgment. This work is supported by JSPS Grant-in-Aid for Scientific Research No. 25220001 and Grant-in-Aid for JSPS Fellows No. 02603125.

2 Holonomic system and initial values

Let

$$\Sigma = \text{diag}(\sigma_1^2, \dots, \sigma_d^2), \quad \mu = (\mu_1, \dots, \mu_d)^\top.$$

We define new parameters λ_i, τ_i , $i = 1, \dots, d$, by

$$\lambda_i = -\frac{1}{2\sigma_i^2}, \quad \tau_i = \frac{\mu_i}{\sigma_i^2}$$

and the Fisher-Bingham integral $f(\lambda, \tau, r)$ by

$$f(\lambda, \tau, r) = \int_{S^{d-1}(r)} \exp\left(\sum_{i=1}^d \lambda_i t_i^2 + \sum_{i=1}^d \tau_i t_i\right) d\mathbf{t}, \quad (2)$$

where $\lambda = (\lambda_1, \dots, \lambda_d)$, $\tau = (\tau_1, \dots, \tau_d)$, $S^{d-1}(r) = \{\mathbf{t} \in \mathbf{R}^d \mid t_1^2 + \dots + t_d^2 = r^2\}$ is the sphere of radius r and $d\mathbf{t}$ is the volume element of $S^{d-1}(r)$ so that

$$\int_{S^{d-1}(r)} d\mathbf{t} = r^{d-1} S_{d-1}, \quad S_{d-1} = \text{Vol}(S^{d-1}(1)) = \frac{2\pi^{d/2}}{\Gamma(d/2)}.$$

Then $G(r)$ in (1) is written as

$$G(r) = \frac{\prod_{i=1}^d \sqrt{-\lambda_i}}{\pi^{d/2}} \exp\left(\frac{1}{4} \sum_{i=1}^d \frac{\tau_i^2}{\lambda_i}\right) \int_0^r f(\lambda, \tau, s) ds. \quad (3)$$

We will numerically integrate the right-hand side of (3). We denote the partial differential operator with respect to λ by ∂_λ . For $\mathbf{t} \in S^{d-1}(r)$, $(t_1^2 + \dots + t_d^2)/r^2 = 1$ and

$$\begin{aligned} f(\lambda, \tau, r) &= \int_{S^{d-1}(r)} \frac{1}{r^2} (t_1^2 + \dots + t_d^2) \exp\left(\sum_{i=1}^d \lambda_i t_i^2 + \sum_{i=1}^d \tau_i t_i\right) dt \\ &= \frac{1}{r^2} (\partial_{\lambda_1} + \dots + \partial_{\lambda_d}) f(\lambda, \tau, r). \end{aligned} \quad (4)$$

By HGM we evaluate $\partial_{\lambda_i} f(\lambda, \tau, r)$, $i = 1, \dots, d$, and use (4) to compute $f(\lambda, \tau, r)$. In fact we also evaluate $\partial_{\tau_i} f(\lambda, \tau, r)$, $i = 1, \dots, d$.

Define a $2d$ -dimensional vector of partial derivatives of $f(\lambda, \tau, r)$ by

$$\mathbf{F} = (\partial_{\tau_1} f, \dots, \partial_{\tau_d} f, \partial_{\lambda_1} f, \dots, \partial_{\lambda_d} f)^\top. \quad (5)$$

Elements of \mathbf{F} are called ‘‘standard monomials’’ in HGM. By Theorem 3 of [9] we have

$$\partial_r \mathbf{F} = P_r \mathbf{F}, \quad (6)$$

where the $2d \times 2d$ matrix $P_r = (p_{ij})$, called the Pfaffian matrix, is of the form

$$P_r = \frac{1}{r} \begin{pmatrix} 2r^2\lambda_1 + 1 & \mathbf{O} & \tau_1 & \cdots & \tau_1 \\ & \ddots & & \vdots & \\ \mathbf{O} & & 2r^2\lambda_d + 1 & \tau_d & \cdots & \tau_d \\ r^2\tau_1 & & \mathbf{O} & 2r^2\lambda_1 + 2 & & \mathbf{1} \\ & \ddots & & & \ddots & \\ \mathbf{O} & & r^2\tau_d & \mathbf{1} & & 2r^2\lambda_d + 2 \end{pmatrix}, \quad (7)$$

with \mathbf{O} denoting an off-diagonal block of 0’s and $\mathbf{1}$ denoting an off-diagonal block of 1’s. The elements p_{ij} of P_r are expressed as

$$\begin{aligned} rp_{ij} &= (2\lambda_i r^2 + 1)\delta_{ij} + \sum_{k=1}^d \tau_i \delta_{j(k+d)} \quad (1 \leq i \leq d), \\ rp_{(i+d)j} &= \tau_i r^2 \delta_{ij} + (2\lambda_i r^2 + 2)\delta_{j(i+d)} + \sum_{k \neq i} \delta_{j(k+d)} \quad (1 \leq i \leq d), \end{aligned}$$

for $1 \leq j \leq 2d$, where δ_{ij} denotes Kronecker’s delta. Given initial values for the elements of \mathbf{F} at $r = r_0$, we can apply a standard ODE solver to (6) for numerically evaluating \mathbf{F} .

For the initial values at a small $r = r_0 > 0$, we can use the following series expansion of the Fisher-Bingham integral ([11]):

$$f(\lambda, \tau, r) = r^{d-1} S_{d-1} \times \sum_{\alpha, \beta \in \mathbb{N}_0^d} r^{2|\alpha+\beta|} \frac{(d-2)!! \prod_{i=1}^d (2\alpha_i + 2\beta_i - 1)!!}{(d-2+2|\alpha|+2|\beta|)!! \alpha! (2\beta)!} \lambda^\alpha \tau^{2\beta}, \quad (8)$$

where $\mathbb{N}_0 = \{0, 1, 2, \dots\}$ and for a multi-index $\alpha \in \mathbb{N}_0^d$ we define

$$\alpha! = \prod_{i=1}^d \alpha_i!, \quad \alpha!! = \prod_{i=1}^d \alpha_i!! \text{ and } |\alpha| = \sum_{i=1}^d \alpha_i.$$

By term by term differentiation of this series we can evaluate derivatives of $f(\lambda, \tau, r)$. For computing the initial values, we apply the following approximation:

$$\frac{\partial f}{\partial \tau_i} = S_{d-1} r^{d+1} \tau_i + O(r^{d+3}) \quad (i = 1, \dots, d), \quad (9)$$

$$\frac{\partial f}{\partial \lambda_i} = S_{d-1} r^{d+1} + O(r^{d+3}) \quad (i = 1, \dots, d). \quad (10)$$

By this approximation, we reduce the computational time for the initial values. However the accuracy of the result does not decrease at all as we will show in Section 4.

As $r \rightarrow \infty$, the absolute values of $f(\lambda, \tau, r)$ and its derivatives become exponentially small, as we analyze the behavior in the next section. Hence we also consider the following vector

$$\mathbf{Q} = \exp(-r^2 \lambda_1 - r|\tau_1|) \left(\frac{1}{r} \partial_{\tau_1} f, \partial_{\tau_2} f, \dots, \partial_{\tau_d} f, \frac{1}{r^2} \partial_{\lambda_1} f, \partial_{\lambda_2} f, \dots, \partial_{\lambda_d} f \right)^\top. \quad (11)$$

Then from (6) it is easy to obtain $\partial_r \mathbf{Q}$ as

$$\partial_r \mathbf{Q} = (D^{-1} \partial_r D - (2r \lambda_1 + |\tau_1|) I_{2d} + D P_r D^{-1}) \mathbf{Q}, \quad (12)$$

where I_{2d} is the identity matrix with size $2d$ and

$$D = \text{diag} \left(\frac{1}{r}, 1, \dots, 1, \frac{1}{r^2}, 1, \dots, 1 \right).$$

The equation (11) is a refinement of the equation (21) in [9]. By Proposition 3.1 in the next section, each element of \mathbf{Q} converges to some non-zero value when r goes to the infinity. This prevents the adaptive Runge-Kutta method from slowing down.

3 Laplace approximation close to the infinity

In our implementation of HGM, we start from a small $r = r_0 > 0$ and numerically integrate \mathbf{F} in (5) up to $r = 1$ and then integrate \mathbf{Q} in (11) toward $r = \infty$. In order to assess the accuracy of \mathbf{Q} for large r , we derive the asymptotic values of the elements of \mathbf{Q} by the Laplace method. The Laplace approximation, including higher order terms, for the Fisher-Bingham integral itself was given in [12]. However here we also need approximations for its derivatives, which were not given in [12]. Hence we give the approximations of the main terms of the Fisher-Bingham integral and its derivatives and a sketch of their proofs.

We first consider the case of single largest λ_1 . We state the following result.

Proposition 3.1. *Suppose $0 > \lambda_1 > \lambda_2 \geq \dots \geq \lambda_d$. Then, as $r \rightarrow \infty$,*

$$f(\lambda, \tau, r) = \frac{\pi^{(d-1)/2}}{\prod_{i=2}^d (\lambda_1 - \lambda_i)^{1/2}} (e^{r\tau_1} + e^{-r\tau_1}) \exp\left(r^2 \lambda_1 - \sum_{i=2}^d \frac{\tau_i^2}{4(\lambda_i - \lambda_1)}\right) (1 + o(1)). \quad (13)$$

$$\partial_{\lambda_1} f(\lambda, \tau, r) = r^2 f(\lambda_1, \tau_1, r) (1 + o(1)), \quad (14)$$

$$\partial_{\lambda_j} f(\lambda, \tau, r) = \left\{ \left(\frac{\tau_j}{2(\lambda_j - \lambda_1)} \right)^2 + \frac{1}{2(\lambda_1 - \lambda_j)} \right\} f(\lambda, \tau, r) (1 + o(1)), \quad (j = 2, \dots, d) \quad (15)$$

$$\partial_{\tau_1} f(\lambda, \tau, r) = r \frac{e^{r\tau_1} - e^{-r\tau_1}}{e^{r\tau_1} + e^{-r\tau_1}} f(\lambda, \tau, r) (1 + o(1)), \quad (16)$$

$$\partial_{\tau_j} f(\lambda, \tau, r) = \frac{\tau_j}{2(\lambda_1 - \lambda_j)} f(\lambda, \tau, r) (1 + o(1)), \quad (j = 2, \dots, d). \quad (17)$$

Note that for $\tau_1 > 0$, in (13) $e^{-r\tau_1}$ is exponentially smaller than $e^{r\tau_1}$ and it can be omitted. However we leave $e^{-r\tau_1}$ there for consistency with the case of $\tau_1 = 0$. Also we found that leaving $e^{-r\tau_1}$ in (13) greatly improves the approximation.

We now give a rough proof of Proposition 3.1. In the proof, the main contributions from the neighborhoods of maximal points are carefully evaluated, but the contributions from outside the neighborhoods are not bounded rigorously. Replacing t_i by rt_i and integrating over $S^{d-1}(1)$ can write

$$f(\lambda, \tau, r) = r^{d-1} \int_{S^{d-1}(1)} \exp\left(r^2 \sum_{i=1}^d \lambda_i t_i^2 + r \sum_{i=1}^d \tau_i t_i\right) dt, \quad (18)$$

$$\partial_{\lambda_j} f(\lambda, \tau, r) = r^{d+1} \int_{S^{d-1}(1)} t_j^2 \exp\left(r^2 \sum_{i=1}^d \lambda_i t_i^2 + r \sum_{i=1}^d \tau_i t_i\right) dt, \quad (19)$$

$$\partial_{\tau_j} f(\lambda, \tau, r) = r^d \int_{S^{d-1}(1)} t_j \exp\left(r^2 \sum_{i=1}^d \lambda_i t_i^2 + r \sum_{i=1}^d \tau_i t_i\right) dt. \quad (20)$$

For very large r

$$r^2(\lambda_1 t_1^2 + \lambda_2 t_2^2 + \dots + \lambda_d t_d^2), \quad 1 = t_1^2 + \dots + t_d^2, \quad (21)$$

takes its maximum value at two points $t_1 = \pm 1, t_2 = \dots = t_d = 0$. The main contributions to (18)–(20) come from neighborhoods of these two points $(\pm 1, 0, \dots, 0)$. The contribution from the complement of these two neighborhoods should be exponentially small as $r \rightarrow \infty$, although we do not give a detailed argument. We also have to consider the effect of $r \sum_{i=1}^d \tau_i t_i$. But it is of the order $O(r)$, whereas (21) is of the order $O(r^2)$. Hence $r \sum_{i=1}^d \tau_i t_i$ only perturbs the maximizing values $(\pm 1, 0, \dots, 0)$ by the term of the order $O(1/r)$. Based on these considerations write

$$t_1^2 = 1 - t_2^2 - \dots - t_d^2, \quad t_1 = \pm \sqrt{1 - t_2^2 - \dots - t_d^2} \doteq \pm \left(1 - \frac{1}{2}(t_2^2 + \dots + t_d^2)\right),$$

where $|t_2|, \dots, |t_d|$ are small. As shown below, $|t_i|, i = 2, \dots, d$, are of the order $O(1/r)$. We now

consider the neighborhood of $(1, 0, \dots, 0)$. By completing the squares we have

$$\begin{aligned}
& r^2 \sum_{i=1}^d \lambda_i t_i^2 + r \sum_{i=1}^d \tau_i t_i \\
&= r^2 \lambda_1 + r \tau_1 + r^2 \sum_{i=2}^d \left((\lambda_i - \lambda_1 - \frac{\tau_1}{2r}) t_i^2 + \frac{\tau_i}{r} t_i \right) + o(1) \\
&= r^2 \lambda_1 + r \tau_1 + \sum_{i=2}^d \left[(\lambda_i - \lambda_1 - \frac{\tau_1}{2r}) \left(r t_i + \frac{\tau_i}{2(\lambda_i - \lambda_1 - \frac{\tau_1}{2r})} \right)^2 - \frac{\tau_i^2}{4(\lambda_i - \lambda_1 - \frac{\tau_1}{2r})} \right] + o(1) \quad (22) \\
&= r^2 \lambda_1 + r \tau_1 + \sum_{i=2}^d \left[(\lambda_i - \lambda_1) \left(r t_i + \frac{\tau_i}{2(\lambda_i - \lambda_1)} \right)^2 - \frac{\tau_i^2}{4(\lambda_i - \lambda_1)} \right] + o(1).
\end{aligned}$$

Furthermore around $(1, 0, \dots, 0)$ the volume element $d\mathbf{t}$ of the unit sphere $S^{d-1}(1)$ is approximately equal to the Lebesgue measure $dt_2 \dots dt_d$, with the error of the order $t_2^2 + \dots + t_d^2$. Hence by the change of variables

$$u_i = r t_i, \quad i = 2, \dots, d,$$

the contribution to $f(\lambda, \tau, r)$ from the neighborhood of $(1, 0, \dots, 0)$ is evaluated as

$$\begin{aligned}
& \exp(r^2 \lambda_1 + r \tau_1) \int_{\mathbb{R}^{d-1}} \exp\left((\lambda_i - \lambda_1) \left(u_i + \frac{\tau_i}{2(\lambda_i - \lambda_1)} \right)^2 - \frac{\tau_i^2}{4(\lambda_i - \lambda_1)} \right) du_1 \dots du_d \\
&= \exp\left(r^2 \lambda_1 + r \tau_1 - \sum_{i=2}^d \frac{\tau_i^2}{4(\lambda_i - \lambda_1)} \right) \frac{\pi^{(d-1)/2}}{\prod_{i=2}^d (\lambda_i - \lambda_1)^{1/2}}. \quad (23)
\end{aligned}$$

Similarly by changing the sign of τ_1 we can evaluate the contribution from the neighborhood of $(-1, 0, \dots, 0)$ as

$$\exp\left(r^2 \lambda_1 - r \tau_1 - \sum_{i=2}^d \frac{\tau_i^2}{4(\lambda_i - \lambda_1)} \right) \frac{\pi^{(d-1)/2}}{\prod_{i=2}^d (\lambda_i - \lambda_1)^{1/2}}. \quad (24)$$

Adding (23) and (24) we obtain (13).

For $\partial_{\lambda_1} f(\lambda, \tau, r)$ and $\partial_{\tau_1} f(\lambda, \tau, r)$, we can just put $t_1 = \pm 1$ in (19) and (20). Adding contributions from two neighborhoods we obtain (14) and (16).

For $\partial_{x_i} f(\lambda, \tau, r)$ and $\partial_{\tau_i} f(\lambda, \tau, r)$, $j \geq 2$, we write

$$\begin{aligned}
t_j &= \frac{u_j}{r} = \frac{1}{r} \left(u_j + \frac{\tau_j}{2(\lambda_j - \lambda_1)} - \frac{\tau_j}{2(\lambda_j - \lambda_1)} \right), \\
t_j^2 &= \frac{1}{r^2} \left(u_j + \frac{\tau_j}{2(\lambda_j - \lambda_1)} - \frac{\tau_j}{2(\lambda_j - \lambda_1)} \right)^2
\end{aligned}$$

and take the expectation with respect to a normal density. Then we obtain (15) and (17). Although we did not give a detailed analysis of the remainder terms, we can show that the relative errors in (14)–(17) are of the order $O(1/r)$. This completes the proof of Proposition 3.1.

A generalization of Proposition 3.1 to the case that $\lambda_1 = \dots = \lambda_m > \lambda_{m+1} \geq \dots \geq \lambda_d$ is given in Appendix. We note that numerically HGM works fine even if some of the λ 's are close to one another, because the Pfaffian system does not have a singular locus except at $r = 0$ and the main exponential order is the same in Proposition 3.1 and in Proposition A.1. However when we want to check whether the ratio of HGM to the asymptotic value is close to one, then we have difficulty when some of the λ 's are close to one another.

4 Numerical experiments

In this section we describe our numerical experiments on the performance of HGM. The programs and the raw data of our numerical experiments are obtained at

<http://github.com/tkoyama-may10/ball-probability/>

Our programs utilize the Gnu Scientific Library[6].

In our experiments we compute the initial values of $r^{-(d+1)}\mathbf{F}$ at $r = r_0 = 1.0 \times 10^{-6}$ by (9) and (10). The reason for multiplying \mathbf{F} by $r^{-(d+1)}$ is that the values of elements of \mathbf{F} are too small at r_0 for floating point numbers. Then up to $r = 1$, we solve the differential equation (6) numerically. In our implementation, we utilize explicit embedded Runge-Kutta Prince-Dormand (8, 9) method and we set the accuracy to 1.0×10^{-6} . In order to prevent the elements of \mathbf{F} becoming too large, we re-scale the elements of \mathbf{F} several times. Then at $r = 1$ we switch to \mathbf{Q} in (11) and solve (12).

Note that we can not take $r = 0$ as an initial point. The point $r = 0$ is in the singular locus of the differential equation (6) since the denominator of P_r becomes zero at the point. Hence, numerical differential equation solvers can not compute the differentiation of \mathbf{F} at the point.

Our implementation computes the initial value of \mathbf{F} by the approximations (9) and (10), which use only the first term of the series expansions. Hence, we have to take very small value for r in order to reduce the error.

Each component of vector \mathbf{F} takes very small value at $r_0 = 10^{-6}$. We deal with this problem by storing not the value of \mathbf{F} itself but the product of \mathbf{F} and a large constant in double precision type array. Related to this problem, there is another problem that the value of each component of \mathbf{F} increases rapidly when we solve ordinary differential equation (6) numerically. We multiply vector \mathbf{F} by a small constant when a component of \mathbf{F} becomes larger than a fixed value. By this way, our implementation prevents values in double precision type array becoming too large.

Our first experiment is for $d = 3$ and the following parameter values

$$\begin{aligned} \sigma_1 &= 3.00, & \sigma_2 &= 2.00, & \sigma_3 &= 1.00, \\ \mu_1 &= 1.00, & \mu_2 &= 0.50, & \mu_3 &= 0.25, \end{aligned} \tag{25}$$

i.e.,

$$\begin{aligned} \lambda_1 &= -0.0555556, & \lambda_2 &= -0.125, & \lambda_3 &= -0.5, \\ \tau_1 &= 0.111111, & \tau_2 &= 0.125, & \tau_3 &= 0.25. \end{aligned}$$

By HGM we compute $G(r)$. We show its graph in Figure 1 to confirm that our implementation correctly calculated the asymptotic behavior as $G(r) \rightarrow 1$ as $r \rightarrow \infty$.

For this example, we also check the accuracy by computing the ratios of $f(\lambda, \tau, r)$ and the elements of \mathbf{F} to their asymptotic expressions in Proposition 3.1. The left figure of Figure 2 shows the ratio of $f(\lambda, \tau, r)$ to its asymptotic expression and the right figure shows the ratios of elements of \mathbf{F} to their asymptotic expressions. Note that the value of the ratio corresponding to $\partial f / \partial \lambda_i$ is very close to that of $\partial f / \partial \tau_i$ so that the triangles overlap with the circles. We see that the numerical integration involved in HGM, starting from a small r_0 , is remarkably accurate, so that the ratios numerically converge to 1 as $r \rightarrow \infty$.

In our second example we consider diagonal matrices $\Sigma^{(1)}$ and $\Sigma^{(2)}$ with diagonal elements

$$(\sigma_k^2)^{(1)} = \frac{d+1}{k(k+1)} \quad (1 \leq k \leq d), \tag{26}$$

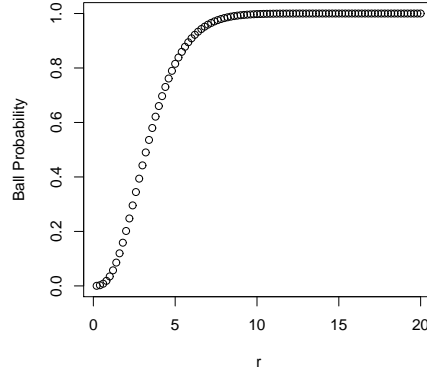


Figure 1: CDF $G(r)$ for the first experiment

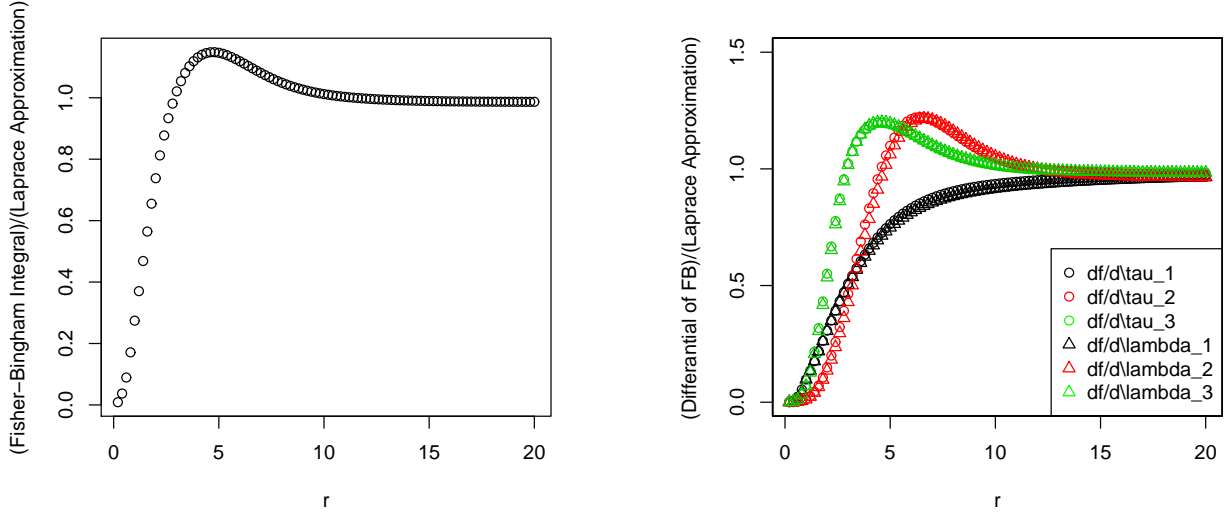


Figure 2: Ratios to the Laplace approximations

and

$$(\sigma_k^2)^{(2)} = \frac{2(d+2)(d+3)}{k(k+1)(k+2)(k+3)} \quad (1 \leq k \leq d), \quad (27)$$

respectively. These weights are considered for cumulative chi-square statistics in [7]. Let

$$\begin{aligned} \mu^{(1)} &= 0, \\ \mu^{(2)} &= (0 \quad 0.01 \quad 0.02 \quad \cdots \quad 0.01 \times (d-1))^\top. \end{aligned}$$

For each dimension d , we computed the probability $P(10^{-6} \leq \|\mathbf{X}\| < 40.0)$ and measured the computational times in seconds. We considered the following four patterns of parameters:

$$\begin{aligned} &(\Sigma^{(1)}, \mu^{(1)}), && (\Sigma^{(1)}, \mu^{(2)}), \\ &(\Sigma^{(2)}, \mu^{(1)}), && (\Sigma^{(2)}, \mu^{(2)}). \end{aligned}$$

The experimental results are shown in Table 1. $1-p$ stands for the values $1-P(10^{-6} \leq \|\mathbf{X}\| < 40.0)$ are generally accurate to 10^{-8} .

Table 1: Accuracy and computational times for $\Sigma^{(1)}$ and $\Sigma^{(2)}$

dimension	$\Sigma^{(1)}$				$\Sigma^{(2)}$			
	$\mu = 0$		$\mu \neq 0$		$\mu = 0$		$\mu \neq 0$	
	$1-p$	times(s)	$1-p$	times(s)	$1-p$	times(s)	$1-p$	times(s)
10	1.60e-08	0.03	1.60e-08	0.03	1.60e-08	0.11	2.10e-09	0.11
11	1.76e-08	0.03	1.57e-08	0.04	1.76e-08	0.12	1.56e-09	0.14
12	1.61e-08	0.04	1.15e-08	0.04	1.61e-08	0.16	9.59e-10	0.17
13	1.81e-08	0.04	1.05e-08	0.04	1.80e-08	0.20	7.90e-10	0.19
14	2.02e-08	0.04	9.95e-09	0.05	2.02e-08	0.24	6.94e-10	0.25
15	2.34e-08	0.04	9.58e-09	0.06	2.34e-08	0.30	6.44e-10	0.30
16	2.77e-08	0.06	9.73e-09	0.07	2.77e-08	0.36	2.89e-10	0.36
17	3.40e-08	0.07	4.85e-09	0.08	3.40e-08	0.41	2.74e-10	0.42
18	1.89e-08	0.08	4.62e-09	0.08	1.89e-08	0.49	2.82e-10	0.52
19	2.08e-08	0.08	4.40e-09	0.10	2.09e-08	0.56	4.05e-10	0.57
20	2.33e-08	0.10	4.32e-09	0.11	2.41e-08	0.65	1.13e-09	0.65

As the radius r increases or the dimension d of the sphere increases, our implementation takes long time to evaluate. Table 1 shows that the computational complexity also depends on the values of λ . However we do not know what value of λ makes the computational time worse.

As our third example we consider how our method works for large dimension. Corresponding to the asymptotic null distribution of Anderson-Darling statistic, which is an infinite sum of weighted χ^2 variables, consider the weights

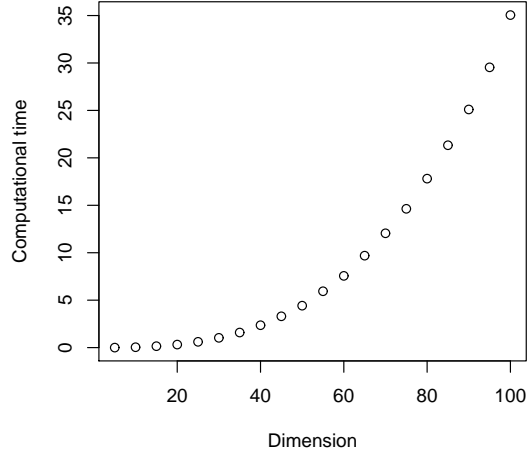
$$\sigma_k^2 = \frac{1}{k(k+1)}, \quad \mu_k = 0 \quad (1 \leq k \leq d).$$

Here we truncate the infinite series at d . We computed the probability and measured its computational time. We fixed the radius as $r = 20.0$. The results on the computational time are shown in Table 2 and its figure. Even for $d = 100$, our method is accurate and fast enough to be practical. This is a remarkable progress since the implementation of HGM in [9] can compute only up to dimension $d = 8$. The key idea for this progress are the simple approximation of the initial values (9) and (10) for HGM and the refined differential equation (12) based on the Laplace approximation.

The computational bottleneck of HGM is the computation of $P_r \mathbf{F}$ in each step of solving the ODE. By the form of the matrix P_r , the number of additions in each step increases in order $O(d^2)$. We guess this is a reason that growth of computational times in the figure of Table 2 seems to be in the order $O(d^2)$.

Table 2: Computational times for Anderson-Darling statistic

dim	$1 - p$	time(s)
30	5.70e-08	1.03
35	3.76e-08	1.59
40	4.85e-08	2.36
45	6.13e-08	3.30
50	8.97e-08	4.42
55	5.29e-08	5.94
60	7.91e-08	7.56
65	6.28e-08	9.69
70	1.02e-07	12.05
75	6.77e-08	14.63
80	7.22e-08	17.81
85	6.25e-08	21.33
90	5.64e-08	25.10
95	5.21e-08	29.54
100	4.90e-08	35.05



Graph of computational times

As our fourth example we consider the case where Σ is the identity matrix and $\mu = 0$. In this case, the Fisher–Bingham integral can be written by the density function of χ -distribution, and we have

$$f(r) = \frac{2\pi^{d/2}}{\Gamma(d/2)} r^{d-1} e^{-r^2/2}.$$

Table 3 shows the result for $f(1.0)$ by HGM and difference $\frac{2\pi^{d/2}}{\Gamma(d/2)} r^{d-1} e^{-r^2/2} - f(1.0)$ for each dimension.

Table 3: Comparison to χ -distribution: $\Sigma = I$ and $\mu = 0$.

dim	hgm	exact–hgm
3	7.621888	1.35e-06
4	11.972435	7.09e-07
5	15.963247	4.85e-07
6	18.806257	3.70e-07
7	20.060008	3.34e-07
8	19.693866	3.13e-07
9	18.005821	2.88e-07
10	15.467527	2.47e-07

As our fifth example we consider the case where

$$\Sigma = \text{diag} \left(\frac{1}{\sqrt{2}}, \frac{1}{\sqrt{2}}, \frac{1}{\sqrt{4}}, \frac{1}{\sqrt{4}}, \frac{1}{\sqrt{6}}, \frac{1}{\sqrt{6}}, \dots, \frac{1}{\sqrt{2n}}, \frac{1}{\sqrt{2n}} \right), \mu = \mathbf{0} \quad (d = 2n).$$

In this case, the ball probability (1) equals to

$$P \left(\frac{1}{2} X_1^2 + \frac{1}{2} X_2^2 + \frac{1}{4} X_3^2 + \frac{1}{4} X_4^2 + \frac{1}{6} X_5^2 + \frac{1}{6} X_6^2 + \dots + \frac{1}{2n} X_{2n-1}^2 + \frac{1}{2n} X_{2n}^2 < r^2 \right)$$

where X_1, \dots, X_{2n} are independent and identically distributed with the standard normal distribution. Since the distribution of $\frac{1}{2k}(X_{2k-1}^2 + X_{2k}^2)$ is the exponential distribution with the rate parameter k , the above probability is equal to $(1 - e^{-r^2})^n$ [5, p.21]. The second column in Table 4 shows the result of HGM for the ball probability at $r = 1.0$. The third column shows the difference between HGM and the exact value.

Table 4: Comparison at specific parameters.

dim	hgm	exact-hgm
6	0.252580	4.97e-09
8	0.159661	2.54e-09
10	0.100925	1.61e-09
12	0.063797	1.03e-09
14	0.040327	8.16e-10
16	0.025492	7.07e-10
18	0.016114	3.04e-10
20	0.010186	2.37e-10

5 Summary and discussion

In this paper we applied HGM for computing distribution function of a weighted sum of independent noncentral chi-square random variables. We found that our method is numerically both accurate and fast, after we implemented the following ideas. First, during the application of Runge-Kutta method, we re-scaled the vector \mathbf{F} in (5) as needed to keep its elements within the precision for floating point numbers. Also we divided the interval for integration into $(0, 1]$ and $[1, \infty)$ and switched from \mathbf{F} to \mathbf{Q} in (11) in view of the asymptotic values for \mathbf{Q} . Our experience in this paper shows that re-scaling of the standard monomials is important in numerical implementation of HGM.

In our implementation, the numerical integration starts from a small $r = r_0 > 0$ and the integration proceeds to $r = \infty$. On the other hand, we have asymptotic results for large r in Section 3. Then we might consider reversing the direction of integration and start with initial values at very large r . We may call the former the “forward integration” and the latter the “backward integration”. However we found that the backward integration is not numerically stable. Hence the asymptotic values can not be used as initial values. In this paper we used the asymptotic values just for checking the accuracy HGM in the forward direction.

It is an interesting question, whether the asymptotic values can be used to adjust the values of the forward integration. We may look at the difference between \mathbf{F} by forward HGM and its asymptotic value for very large r and use the difference to adjust \mathbf{F} at intermediate values of r . However it is not clear how this adjustment can be implemented.

A A general form of Proposition 3.1

In Proposition 3.1 we assumed $\lambda_1 > \lambda_2$. In this appendix we state the following proposition for the general case $\lambda_1 = \dots = \lambda_m > \lambda_{m+1}$ without a proof. For this case, the integrand for the Fisher-

Bingham integral takes its maximum on the $(m - 1)$ -dimensional sphere $S^{m-1}(1)$, rather than on a finite number of points. However by appropriate choice of coordinates and by multiplication of the volume $\text{Vol}(S^{m-1}(1))$, the derivation of Proposition A.1 is basically the same as Proposition 3.1.

Proposition A.1. *Assume that*

$$0 > \lambda_1 = \dots = \lambda_m > \lambda_{m+1} \geq \dots \geq \lambda_d.$$

If $0 = \tau_1 = \dots = \tau_m$, then as $r \rightarrow \infty$,

$$f(\lambda, \tau, r) = r^{m-1} S_{m-1} \exp \left(r^2 \lambda_1 - \sum_{i=m+1}^d \frac{\tau_i^2}{4(\lambda_i - \lambda_1)} \right) \frac{\pi^{(d-m)/2}}{\prod_{i=m}^d (\lambda_1 - \lambda_i)^{1/2}} (1 + o(1)),$$

$$\partial_{\lambda_j} f(\lambda, \tau, r) = \frac{r^2}{m} f(\lambda, \tau, r) (1 + o(1)), \quad j \leq m,$$

$$\partial_{\tau_j} f(\lambda, \tau, r) = 0, \quad j \leq m,$$

$$\partial_{\tau_j} f(\lambda, \tau, r) = -\frac{\tau_j}{2(\lambda_j - \lambda_1)} f(\lambda, \tau, r) (1 + o(1)), \quad j > m,$$

$$\partial_{\lambda_j} f(\lambda, \tau, r) = \left(\frac{1}{2(\lambda_1 - \lambda_j)} + \frac{\tau_j^2}{4(\lambda_j - \lambda_1)^2} \right) f(\lambda, \tau, r) (1 + o(1)), \quad j > m.$$

If $(\tau_1, \dots, \tau_m) \neq (0, \dots, 0)$, define $\gamma = (\tau_1^2 + \dots + \tau_m^2)^{1/2}$. Then, as $r \rightarrow \infty$,

$$f(\lambda, \tau, r) = \exp \left(r^2 \lambda_1 + r\gamma - \sum_{i=m+1}^d \frac{\tau_i^2}{4(\lambda_i - \lambda_1)} \right) \left(\frac{2r}{\gamma} \right)^{(m-1)/2} \frac{\pi^{(d-1)/2}}{\prod_{i=m}^d (\lambda_1 - \lambda_i)^{1/2}} (1 + o(1)),$$

$$\partial_{\tau_j} f(\lambda, \tau, r) = r \frac{\tau_j}{\gamma} f(\lambda, \tau, r) (1 + o(1)), \quad \tau_j \neq 0, \quad j \leq m,$$

$$\partial_{\lambda_j} f(\lambda, \tau, r) = r^2 \frac{\tau_j^2}{\gamma^2} f(\lambda, \tau, r) (1 + o(1)), \quad \tau_j \neq 0, \quad j \leq m,$$

$$\partial_{\tau_j} f(\lambda, \tau, r) = 0, \quad \tau_j = 0, \quad j \leq m,$$

$$\partial_{\lambda_j} f(\lambda, \tau, r) = \frac{r}{\gamma} f(\lambda, \tau, r) (1 + o(1)), \quad \tau_j = 0, \quad j \leq m,$$

$$\partial_{\tau_j} f(\lambda, \tau, r) = -\frac{\tau_j}{2(\lambda_j - \lambda_1)} f(\lambda, \tau, r) (1 + o(1)), \quad j > m,$$

$$\partial_{\lambda_j} f(\lambda, \tau, r) = \left(\frac{1}{2(\lambda_1 - \lambda_j)} + \frac{\tau_j^2}{4(\lambda_j - \lambda_1)^2} \right) f(\lambda, \tau, r) (1 + o(1)), \quad j > m.$$

References

- [1] T. W. Anderson and D. A. Darling. Asymptotic theory of certain “goodness of fit” criteria based on stochastic processes. *Ann. Math. Statistics*, 23:193–212, 1952.
- [2] A. Castaño-Martínez and F. López-Blázquez. Distribution of a sum of weighted noncentral chi-square variables. *Test*, 14(2):397–415, 2005.
- [3] A. M. Cohen. *Numerical Methods for Laplace Transform Inversion*, volume 5 of *Numerical Methods and Algorithms*. Springer, New York, 2007.

- [4] R. B. D'Agostino and M. A. Stephens, editors. *Goodness-of-Fit Techniques*, volume 68 of *Statistics: Textbooks and Monographs*. Marcel Dekker Inc., New York, 1986.
- [5] W. Feller. *An Introduction to Probability Theory and its Applications. Vol. II*. John Wiley & Sons Inc., 1966.
- [6] GSL. GNU scientific library. <http://www.gnu.org/software/gsl/>, 2015.
- [7] C. Hirotsu. Cumulative chi-squared statistic as a tool for testing goodness of fit. *Biometrika*, 73(1):165–173, 1986.
- [8] T. Koyama. A holonomic ideal which annihilates the Fisher-Bingham integral. *Funkcial. Ekvac.*, 56(1):51–61, 2013.
- [9] T. Koyama, H. Nakayama, K. Nishiyama, and N. Takayama. Holonomic gradient descent for the Fisher-Bingham distribution on the d -dimensional sphere. *Computational Statistics*, 29(3-4):661–683, 2014.
- [10] T. Koyama, H. Nakayama, K. Nishiyama, and N. Takayama. The holonomic rank of the Fisher-Bingham system of differential equations. *J. Pure Appl. Algebra*, 218(11):2060–2071, 2014.
- [11] A. Kume and S. G. Walker. On the Fisher-Bingham distribution. *Stat. Comput.*, 19(2):167–172, 2009.
- [12] A. Kume and A. T. A. Wood. Saddlepoint approximations for the Bingham and Fisher-Bingham normalising constants. *Biometrika*, 92(2):465–476, 2005.
- [13] V. N. Nair. On testing against ordered alternatives in analysis of variance models. *Biometrika*, 73(2):493–499, 1986.
- [14] H. Nakayama, K. Nishiyama, M. Noro, K. Ohara, T. Sei, N. Takayama, and A. Takemura. Holonomic gradient descent and its application to the Fisher-Bingham integral. *Advances in Applied Mathematics*, 47:639–658, 2011.
- [15] T. Sei and A. Kume. Calculating the normalising constant of the Bingham distribution on the sphere using the holonomic gradient method. *Stat. Comput.*, 25(2):321–332, 2015.
- [16] K. Tanaka. *Time Series Analysis: Nonstationary and Noninvertible Distribution Theory*. Wiley Series in Probability and Statistics: Probability and Statistics. John Wiley & Sons Inc., New York, 1996.